CSIRO PUBLISHING

International Journal of Wildland Fire **2021**, *30*, 823–835
https://doi.org/10.1071/WF21045

Characterisation of initial fire weather conditions for large spring wildfires in Alberta, Canada

Cordy Tymstra[A,C], *Piyush Jain*[B] *and Mike D. Flannigan*[A]

[A]Department of Renewable Resources, University of Alberta, 751 General Services Building, Edmonton, AB, T6G 2H1, Canada.
[B]Natural Resources Canada, Canadian Forest Service, Northern Forestry Centre, 5320 122 Street, NW, Edmonton, AB, T6H 3S5, Canada.
[C]Corresponding author. Email: cordy.tymstra@ualberta.ca

Abstract. We evaluated surface and 500-hPa synoptic weather patterns, and fire weather indices from the Canadian Forest Fire Danger Rating System for 80 large wildfires during 1990–2019 in Alberta that started in May and grew to over 1000 ha. Spread days were identified during the first 4 days of wildfire activity. We observed two distinct synoptic weather patterns on these days. Pre-frontal and frontal passage activity was the predominant feature associated with 48% of the calendar spread days. Strong south–south-east winds from a surface high centred east of Alberta (west of Hudson Bay) and supported by an upper ridge, and a surface low located south-west of the ridge occurred on 26% of the calendar spread days. Surface analysis indicates the spring wildfire season in Alberta is driven by very high to extreme Initial Spread Index, a rating of the expected wildfire rate of spread based on Fine Fuel Moisture Code and wind. Very high to extreme values of Buildup Index, a rating of the amount of fuel available for consumption, are not a prerequisite for large wildfires in May. For Alberta, this means large wildfires in May can occur after only a few days of dry, windy weather.

Keywords: wildfire spread, spring boreal wildfires, synoptic weather patterns, fire danger.

Received 8 April 2021, accepted 27 August 2021, published online 16 September 2021

Introduction

Very large wildfires are a common feature of the boreal fire regime in Canada (Tymstra 2015; Hanes *et al.* 2019). However, since 1959, Canada has experienced an increase in the number of lightning wildfires (Coogan *et al.* 2019), area burned (Hanes *et al.* 2019) and the number of wildfire disasters causing evacuations and structural losses (Tymstra *et al.* 2020). Recent disastrous wildfire seasons in western Canada occurred in 2011 (Alberta), 2014 (Northwest Territories), 2015 (Alberta and Saskatchewan), 2016 (Alberta), 2017 and 2018 (British Columbia), and 2019 (Alberta). Projected higher temperatures, more lightning and weather extremes (Flannigan *et al.* 2009; Coogan *et al.* 2019) will contribute to increasing wildfire intensities in the future, and diminishing returns on investment from suppression efforts (Wotton *et al.* 2017). During the 2005–2014 period, extreme wildfire risk increased an estimated 150% to 600% in western Canada as a result of the combined impact of anthropogenic and natural forcing compared with natural variability alone (Kirchmeier-Young *et al.* 2017).

Climate change impacts also include changes in spring phenology resulting in earlier spring wildfire seasons (Beaubien and Hamann 2011; Pickell *et al.* 2017). Spring wildfires across Canada are particularly a challenge during the period between snowmelt and green-up when suppression resources may not yet be fully available, and low fuel moisture levels contribute to extreme wildfire behaviour. In Alberta, spring is the critical season (Tymstra *et al.* 2019) when nearly all of the associated structural losses occur from wildfires. There is therefore great interest in understanding the environmental conditions contributing to wildfires that start in spring, subsequently grow large and become challenging to manage.

Various multivariate approaches have been used to investigate biophysical factors associated with wildfires (occurrence and area burned) in, for example, France (Ganteaume and Jappiot 2013), Spain (Verdú *et al.* 2012; Viedma *et al.* 2015), Portugal (Parente *et al.* 2016), the United States (Parks *et al.* 2018) and Canada (Cumming 2001; Krawchuk *et al.* 2006).

In their investigation of the relationship of various meteorological variables to area burned in Canada, Flannigan and Harrington (1988) found the strongest predictor of the variance in area burned was the duration of dry periods. Earlier studies recognised the importance of wind, Byram (1954) suggesting certain wind profiles are associated with blow-up wildfires, and Schaefer (1957) linking jet streams and wildfires.

Schroeder *et al.* (1964) identified critical synoptic weather types associated with periods of extreme fire behaviour, and Brotak and Reifsnyder (1977) extended similar weather analyses to investigate 60 major wildfires in the eastern United States.

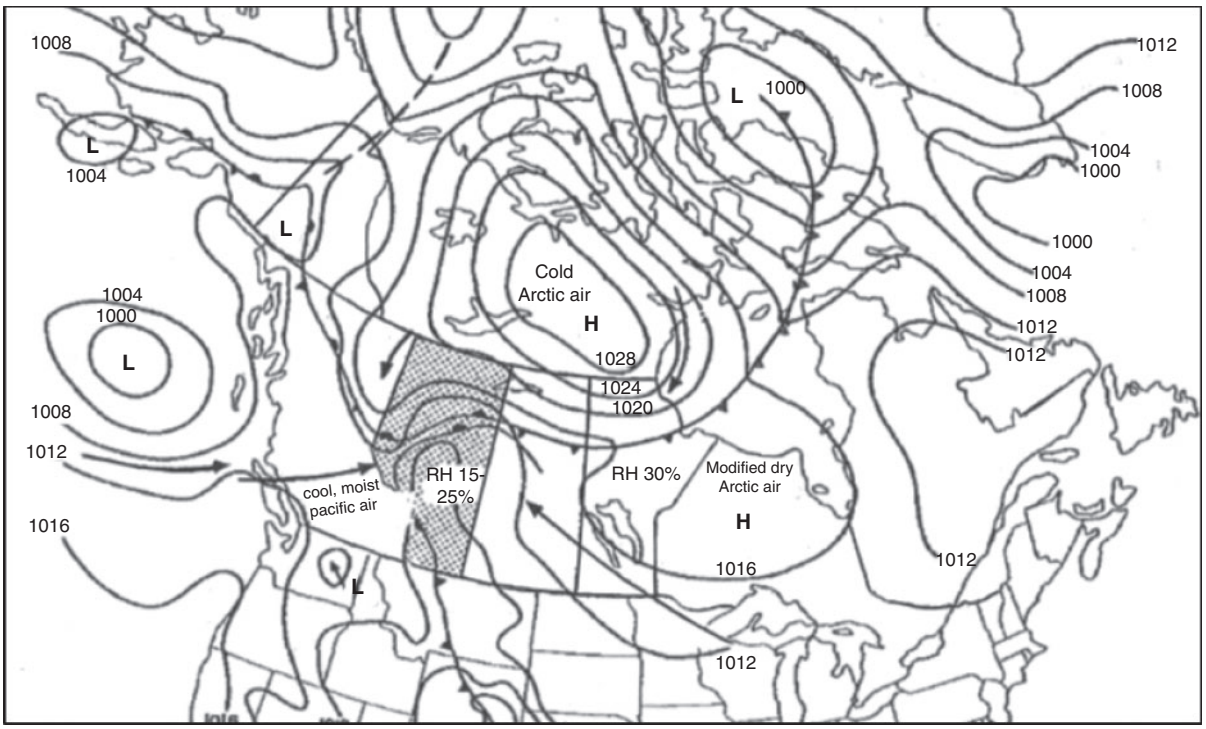

Fig. 1. Surface weather analysis 23 May 1968, 1300 Mountain Standard Time (MST) (2000 Greenwich Mean Time (GMT)). Note the location of the high-pressure area west of Hudson Bay that resulted in a strong, dry, south-east anti-cyclonic flow over central Alberta, and the low-pressure area west of the province with a cyclonic flow supporting the south-east flow. Modified from Kiil and Grigel (1969).

Frontal passages were a common factor for 45 of these wildfires. Skinner *et al.* (2002) found an association between large areas burned in western Canada with 500-hPa ridging, and the mean 500-hPa height difference between 45°N and 65°N latitude. In Alberta, frontal passages are often associated with the breakdown of these 500-hPa ridges and the subsequent arrival of lightning-caused wildfires (Nimchuk 1983).

More recent studies have applied statistical approaches for synoptic weather typing using interpolated geospatial gridded data from meteorological observations or modelled reanalysis products and then correlating these with fire danger metrics. Examples include the use of composite map analysis using National Centers for Environmental Protection/National Center for Atmospheric Research (NCEP/NCAR) reanalysis outputs of days with highest area burned (Pereira *et al.* 2005), correlation analysis of NCEP/NCAR reanalysis outputs and the Haines Index and Palmer Drought Index (Trouet *et al.* 2009), fuzzy c-means cluster analysis classification of fire days into synoptic weather groups (Duane and Brotons 2018); k-means cluster analysis classification of weather type (Ruffault *et al.* 2017); and Self-Organised Map classification of synoptic weather patterns associated with critical fire weather conditions (Crimmins 2006; Lagerquist *et al.* 2017; Zhong *et al.* 2020).

We similarly investigate the association between meteorological variables and synoptic conditions but focus on May wildfire activity in Alberta, Canada. Our attention to the month of May is motivated not only by recent disastrous spring seasons but also past events such as the 'Seven Days in May' wildfire outbreak in 1968 (McLean and Coulcher 1968) when a persistent blocking pattern aloft allowed a surface high to sustain strong and dry south–south-east winds over central Alberta (Fig. 1).

The study area is depicted in Fig. 2. Only those wildfires within the boreal forest in Alberta during the 1990–2019 period were included in the present study. This period was selected because detailed wildfire report and weather data in the Fire Information and Resource Environment System (FIRES), which is managed by Alberta's Wildfire Management Branch (WMB), begins in 1990. The WMB is responsible for managing wildfires on provincial forested lands. Wildfires in the national parks are managed separately and were excluded because of the absence of detailed daily wildfire data similar to that available in Alberta. Wildfire report data from FIRES are available publicly (https://wildfire.alberta.ca/resources/), and weather data are available via a request to the WMB. The next section describes the data and analysis methods used to characterise the fire weather conditions of large spring wildfires in May. This is followed by the results and discussion sections. Our discussion focuses on the operational implications for wildfire behaviour analysts working on incident management teams. The conclusion summarises the key results, limitations and research gaps, and opportunities for enhanced wildfire preparedness in the spring.

Study area

Alberta is the sixth largest province of Canada, landlocked by British Columbia to the west, Saskatchewan to the east, Northwest Territories to the north, and the state of Montana, USA (not included on Fig. 2) to the south. There are five ecozones in Alberta: Prairies, Montane Cordillera, Boreal Plains, Taiga Plains and Taiga Shield (Wiken 1986). The Boreal Plains

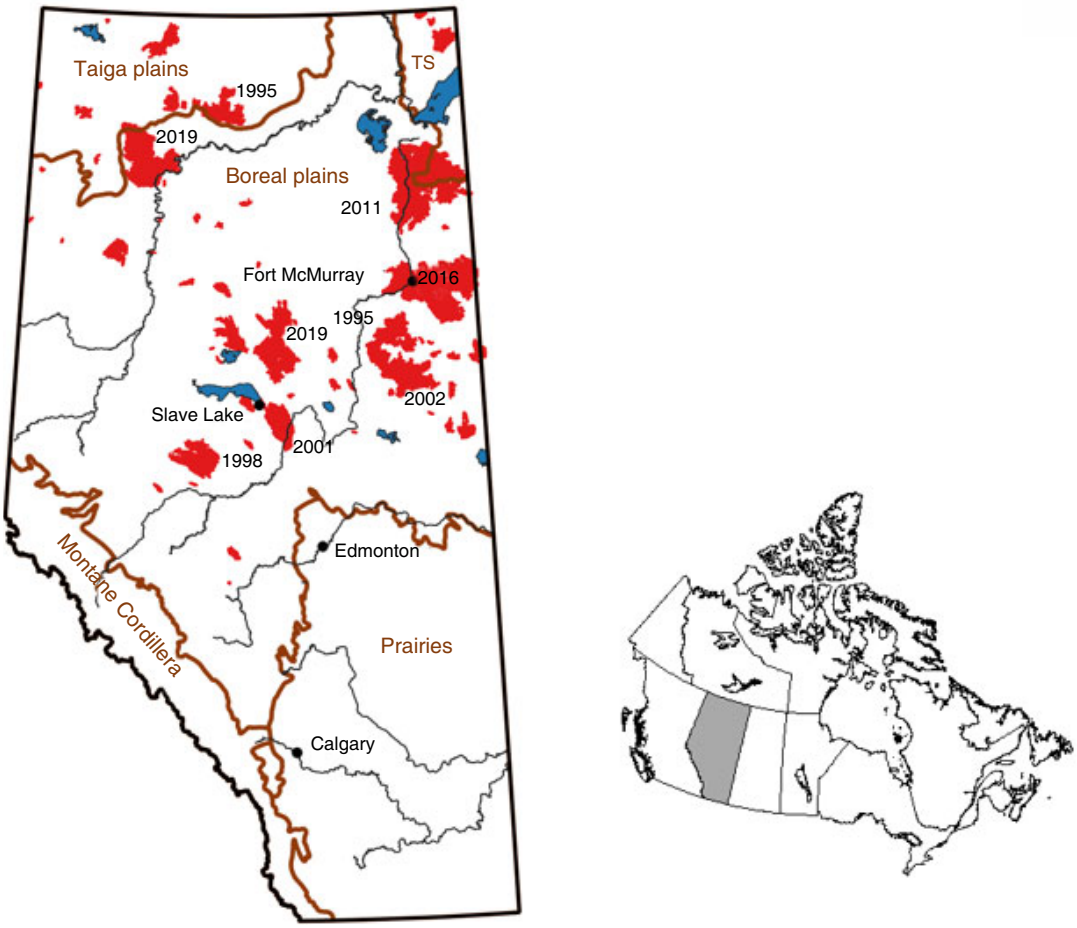

Fig. 2. Location of the Province of Alberta and wildfires greater than 1000 ha in size on provincial forested lands that started during the month of May. Wildfires greater than 100 000 ha are labelled by year. The five ecozones in Alberta are delineated and labelled. TS, Taiga Shield Ecozone. Wildfire perimeter data provided by the Wildfire Management Branch.

Ecozone covers most of Alberta's forested landscape and extends east into Saskatchewan and Manitoba. It is a landscape dominated by coniferous forests interspersed with peatlands (bogs, fens and swamps).

Alberta's geographic location and topographic features influence weather patterns, which impacts the wildfire season. The Rocky Mountains and foothills traversing north-west from the Canada–United States border (49°N) to near Grande Prairie (55°N) support the formation of clouds and precipitation during easterly upslope wind flows, and warming and drying during westerly downslope wind flows. North of Grande Cache, moist Pacific air masses have fairly easy entry into central and northern Alberta. Air masses originating from the Arctic also move unimpeded as they travel south and south-east into the Prairie Provinces (Alberta, Saskatchewan and Manitoba).

Methods

For the 1990–2019 period, we selected all May wildfire starts in Alberta with a reported extinguished size exceeding 1000 ha (see Fig. 2). Point attribute and perimeter data were obtained from the Alberta WMB in Edmonton, Alberta. If a wildfire in Alberta grows larger than 2.0 ha before initial attack begins, it is considered an initial attack (IA) escape. If a wildfire cannot be contained at 1000 hours on the following day when it was assessed, it is reported as a containment or Being Held (BH) escape. Of the selected 80 wildfires, 57 escaped both IA and BH, and 4 escaped IA but were successfully contained (BH success). Despite initial attack resources arriving on 19 wildfires before they exceeded 2 ha in size, BH success was attained on only one wildfire.

Most wildfires are assessed the day they are reported, which typically is the day they started. We focus on the first 4 days, which includes the wildfire start date. For the three wildfires starting earlier but discovered and reported later, and the three wildfires with start dates reported as unknown, we used the discovered date as Day 1. Podur and Wotton (2011) used an Initial Spread Index (ISI) classification threshold of ≥8.7 to differentiate wildfire spread days from non-spread days. ISI is a numerical rating of a wildfire's spread potential (Van Wagner 1987). To derive spread day distributions for input into burn probability modelling, Parisien *et al.* (2013) applied a calculated rate of spread threshold of ≥1 m min^{-1} to identify spread days.

Table 1. Hazard rating classes for fire weather index codes and indices used in Alberta

FFMC, Fine Fuel Moisture Code; DMC, Duff Moisture Code; DC, Drought Code; ISI, Initial Spread Index; BUI, Buildup Index; FWI, Fire Weather Index

Hazard Rating	FFMC	DMC	DC	ISI	BUI	FWI
Low	0–76	0–21	0–79	0–1.5	0–24	0–4.5
Moderate	77–84	22–27	80–189	2–4	25–40	4.5–10.5
High	85–88	28–40	190–299	5–8	41–60	10.5–18.5
Very High	89–91	41–60	300–424	9–15	61–89	18.5–29.5
Extreme	92+	61+	425+	16+	90+	29.5+

Table 2. Synoptic-scale weather patterns and associated pre-frontal, frontal passage and gust occurrences for the 149 spread day events associated with one or more wildfires

For example, a total of 26 spread day events occurred with weather pattern 1a (trough at the surface and a ridge at 500 hPa), 4 days had pre-frontal activity (3 with reported gusts), 8 days had frontal passage (7 with reported gusts), and 11 days had gusts but with no pre-frontal or frontal passage activity

Synoptic-scale weather pattern	Surface + upper (500 hPa) weather pattern	Number of spread day events			
		Total	Pre-frontal/gusts	Frontal passage/gusts	Gusts
Trough/low + ridge/high	1a: Trough + ridge	26	4/3	8/7	11
	1b: Trough + high	1	0	1/1	0
	1c: Low + ridge	32	2/1	17/8	9
	1d: Low + high	2	0	0	0
Trough/low + trough/low	2a: Trough + trough	5	0	4/1	0
	2b: Trough + low	3	0	1/1	1
	2c: Low + trough	1	0	1/1	0
	2d: Low + low	1	0	0	0
Trough/low + other	3a: Trough + col	5	0	0	3
	3b: Trough + zonal	1	0	0	1
	Flow	1	0	0	1
	3c: Low + other				
Ridge/high + ridge/high	4a: Ridge + ridge	12	1/1	2/2	6
	4b: Ridge + high	0	0	0	0
	4c: High + ridge	40	5/2	6/3	18
	4d: High + high	2	0	0	2
Ridge/high + trough/low	5a: Ridge + trough	0	0	0	0
	5b: Ridge + low	0	0	0	0
	5c: High + trough	4	0	2/2	1
	5d: High + low	2	0	2/0	0
Ridge/high + other	6a: Ridge + col	1	0	1/0	0
	6b: High + zonal flow	4	0	0	3
	6c: High + col	2	0	1/1	0
Other + ridge	7a: Col + ridge	3	0	1/1	0
Other + other	8a: Col + col	1	0	0	1

We chose a mixed approach to identify a spread day event. A spread day occurred on Day 1 if the reported wildfire size exceeded 200 ha or the noon ISI was 9 or greater. Spread days occurred on Days 2 to 4 if either they doubled in size from the previous day or the ISI $\geq$ 9 threshold was reached. The ISI threshold of 9 is the start of the Very High ISI category used in Alberta (Table 1). Days with a reported BH or UC (under control) status were not considered as spread days.

We analysed surface (3-h intervals) and 500-hPa synoptic weather patterns (2× per day) for the first 4 days for all 80 wildfires. For those days when a spread event occurred, we manually characterised the weather patterns into 24 surface and upper weather pattern combinations (see Table 2). Ridges and troughs were identified as elongated areas of high (ridge) or low (trough) pressure occurring at the surface or aloft. We identified air masses that were more concentric in shape as lows or highs. The weather pattern 'other' includes col (neutral) and zonal flow.

For the 1990–2004 period, we accessed surface maps from the National Oceanic and Atmospheric Administration (NOAA) National Centers for Environmental Prediction (NCEP) surface analysis archive (National Oceanic and Atmospheric Administration 2021*a*), and 500-hPa maps from the NOAA Central Library weather and climate collections (National Oceanic and Atmospheric Administration 2021*b*). To address gaps in the surface maps during the 1990–2004 period, we also accessed daily surface weather maps from the NOAA central library weather and climate collections (National Oceanic and Atmospheric Administration 2021*c*).

For the 2005–2019 period, we accessed surface maps from the NOAA NCEP surface analysis archives (National Oceanic and Atmospheric Administration 2021*c*), and 500-hPa maps from the NOAA NCEP daily weather map archives (National Oceanic and Atmospheric Administration 2021*d*).

We used the McElhinny *et al.* (2020) global high-resolution (0.25° × 0.25°) dataset of Fire Weather Index (FWI) System fuel moisture codes and fire behaviour indices that were calculated using surface meteorology data from the ERA5 reanalysis (Mesinger *et al.* 2006) for the 1979–2018 period. For our study, we extended this dataset to include 2019. The Province of Alberta including an edge buffer was clipped from the global dataset between –120.125° and –109.875° longitude and 48.875° and 60.125° latitude. FWI System outputs were calculated using the ERA5 deterministic meteorology outputs of temperature (°C), dewpoint temperature (°C) used to derive relative humidity (%), wind speed (km h^{-1}), and 24-h accumulated precipitation (mm). The standard overwinter Drought Code adjustment was used to derive starting values as described by McElhinny *et al.* (2020).

The FWI system was developed adhering to the World Meteorological Organization reporting standards (Lawson and Armitage 2008). For forecasting purposes, the recommended hourly surface wind speed for use in the FWI system is the average 10-m wind speed over the last 10 min before the hour. In Alberta, this average wind speed is calculated using a sampling frequency of 4 Hz. Maximum (peak) observed wind speeds within the last hour were obtained from the nearest weather station. Peak wind speeds continuing longer than 1 min can significantly impact fire behaviour (Crosby and Chandler 2004), but they are not an input in the calculation of Fine Fuel Moisture Code (FFMC) and ISI. FFMC is a numerical rating of the moisture content of fine fuels and their ease of ignition and flammability (Van Wagner 1987). If gusts are reported, fire behaviour analysts typically increase the input wind speed to calibrate their forecast to match what is observed.

If gusts were reported at a weather station, we converted the 10-min average wind speed to a probable maximum 1-min average wind speed and recalculated the FFMC and ISI values using the adjusted wind speed. The wind speeds were adjusted using a piecewise linear function to approximate the converted metric values of the tabular data published by Crosby and Chandler (2004).

$$\text{For } WS_{10} < 19,\ WS_1 = (1.505954 \times WS_{10}) \times 1.11$$

$$\text{For } WS_{10} \geq 19,\ WS_1 = (WS_{10} + 8) \times 1.11$$

where WS_1, adjusted wind speed; and WS_{10}, 10-min average wind speed (km h^{-1}).

Spread events were spatially and temporally group into 29 lightning-caused and 25 human-caused spread event groups (Fig. 3 boxes *c* and *d*). A 100-km radius centred on the ignition points of lightning-caused wildfires, and a 50-km radius centred on the human-caused wildfire ignition points were used to maximise the grouping of wildfires based on similar start dates and location. The larger radius for lightning-caused wildfires allowed for the inclusion of wildfires with the same start dates and orientation with a cold front passage. The use of spread day event groups facilitated the qualitative analysis of the synoptic weather types associated with the wildfire spread events.

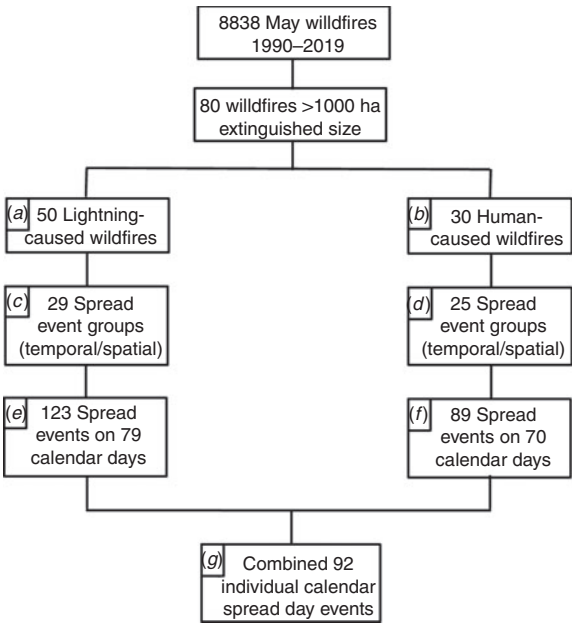

Fig. 3. Calendar day spread event flowchart. The 80 large wildfires are first categorised by cause (boxes *a* and *b*) and then grouped into spatial-temporal spread event groups (boxes *c* and *d*). The total number of spread events are shown in boxes (*e*) and (*f*). The combined number of individual calendar days with one or more spread events is shown in box (*g*).

The 54 groups yielded a total of 212 spread events (boxes *e* and *f* in Fig. 3). Many of the spread events within a group had multiple wildfires occurring on the same day. For example, spread event group 3 (see Table S1, Supplementary material) included 5 wildfires with 15 spread events occurring on 5 separate calendar days. The 212 spread events occurred on 92 individual (unique) calendar day spread events (box *g* in Fig. 3).

We not only investigated the occurrence of synoptic weather patterns similar to those during the 1968 wildfire outbreak during the identified spread event days but also during non-wildfire days. If synoptic weather patterns 4a and 4c (Table 2) with south–southeast winds exceeding 18.5 km h^{-1} (10 knots or a full barb wind speed symbol on weather maps) occurred, it was considered as a potential critical spread day similar to the 1968 wildfire event. The town of Slave Lake was used as a central reference location to cross-validate the wind flow assessed from the surface weather maps using historical hourly weather data for the Slave Lake airport obtained from the Government of Canada historical weather archive (Government of Canada 2021).

Data analysis, including graphics and reported statistical tests, was completed using the *R* software environment (R Core Team 2020), Python programming language (Python Software Foundation (2021), and *Cartopy Python Package* (Met Office 2021).

Results

Wildfire cause, area burned and synoptic weather patterns

Table 2 summarises the synoptic-scale weather patterns and associated pre-frontal, frontal passage and gust occurrences for

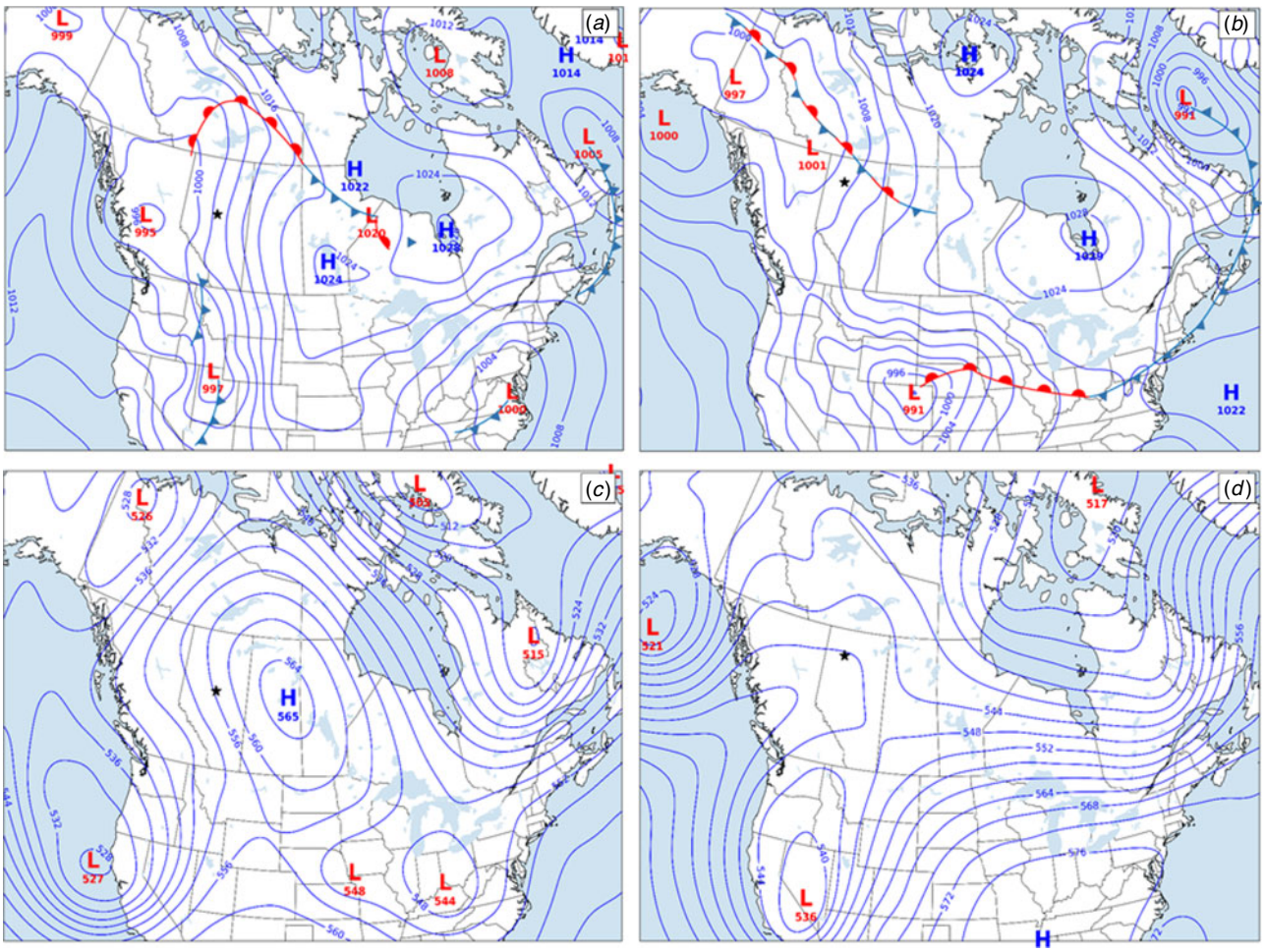

Fig. 4. Surface and 500-hPa analysis on 15 May 2011 (*a*, surface map; *c*, 500-hPa map), and 26 May 2012 (*b*, surface map; *d*, 500-hPa map). Surface maps are 1800 Mountain Daylight Time (MDT) and 500-hPa maps are 0600 MDT. The black star represents the town of Slave Lake (maps *a* and *c*), and Wildfire HF070–2012 (maps *b* and *d*). Wildfire SWF-065–2011 burned through Slave Lake on 15 May. Surface and 500-hPa maps are based on ERA5 model output. Fronts are delineated on the surface maps.

the 149 spread day events (79 lightning and 70 human-caused) during the 1990–2019 period. The two most frequent weather patterns when wildfire spread days occurred are Pattern 1: surface trough or low with an upper ridge or high (41%), and Pattern 4: surface ridge or high with an upper ridge or high (36%), as shown in Table 2. In comparison, of the spread days associated with a surface ridge or high with an upper ridge or high, 67% were due to lightning-caused wildfires. This is due to the higher occurrence of frontal activity, which causes warm air ahead of the advancing cold front to rise and develop cumulus or cumulonimbus clouds and thunderstorms. In comparison, of the spread days associated with a surface ridge or high, with an upper ridge or high, 67% were due to human-caused wildfires. The 149 spread day events fall on 92 individual calendar days (i.e. with one or more wildfires).

Simplified surface and 500-hPa synoptic weather maps were created for illustrative purposes using ERA5 model output. Representative examples of synoptic weather patterns 4a and 4c (Table 2) are shown in Fig. 4. The merging of a cyclonic flow with an anti-cyclonic flow results in a south–south-east wind flow over central and eastern Alberta. These surface patterns are supported by a 500-hPa ridge blocking moist Pacific air masses from entering Alberta. Little to no lightning occurs with synoptic weather patterns 4a and 4c because of the characteristic stable atmospheric conditions. Human-caused wildfires are dominant during these weather patterns.

A continental polar air mass centred west and south-west of Hudson Bay with south–south-east winds over central and eastern Alberta occurred on 10% of all days in May for the 12 years during the 1990–2019 period when no large wildfires started in May (Fig. 5). The occurrence of this synoptic weather pattern increased to 19% during the other 18 years when large wildfires did start in May. During the 92 individual calendar spread days, a Hudson Bay continental polar air mass with a surface low positioned in or near south-west Alberta occurred on ~26% of those days.

Representative examples of synoptic weather patterns 1a and 1c (Table 2) are shown in Fig. 6. These patterns are associated with cold front passages. On 2 May 2016, an upper ridge was centred over Alberta. At the surface, a north–south-oriented cold

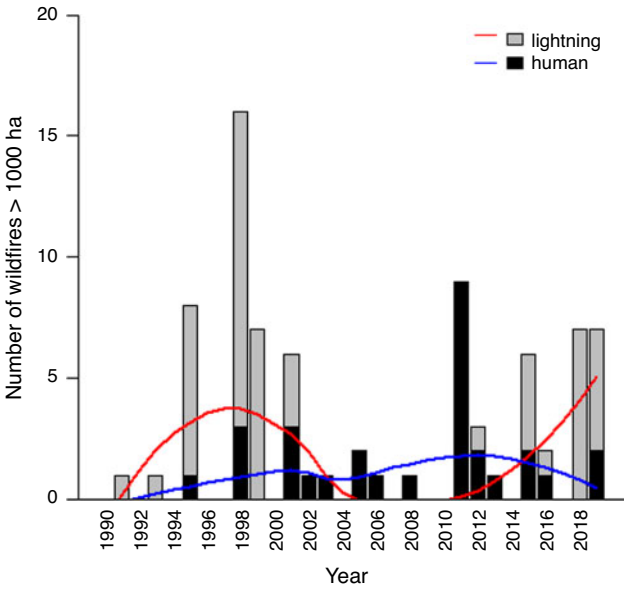

Fig. 5. Annual number of lightning- and human-caused wildfires starting in May and exceeding 1000 ha in extinguished size for the 1990–2019 period. The red and blue lines are locally weighted smoothing outputs.

front positioned along the west coast of British Columbia began tracking eastward on 3 May. The blocking upper ridge moved east on 4 May, allowing the cold front entry into Alberta (Fig. 6*a*). At 1800 MDT, the cold front was positioned just west of the Fort McMurray Urban Service Area. Strong south-west winds ahead of the cold front pushed the 2016 Horse River Wildfire into Fort McMurray. A similar synoptic weather pattern occurred on 17 May 2008 when a cold front passed over wildfire PWF019–2008 (Fig. 6).

Pre-frontal and/or frontal passage activity occurred on 44 (48%) of 92 calendar spread days. In Alberta, these events are often associated with the breakdown of a 500-hPa ridge and increased threat of atmospheric conditions (strong winds and atmospheric instability) conducive to extreme wildfire behaviour (Nimchuk 1983).

In Alberta, wildfire starts in May accounted for 55% of the total extinguished area of all wildfires during the wildfire season (1 March–30 October) for the 1990–2019 period (Fig. 7). For the 80 wildfires that exceeded 1000 ha in size, ~25% of their total extinguished area occurred during the initial 4 days of wildfire growth.

Humans and undetermined causes account for 91% of all May wildfire starts ($n = 8838$) that exceed 0.1 ha in extinguished size. For wildfires greater than 1000 ha during the first decade (1990–1999), lightning was the dominant cause (88%). In the second decade (2000–2009), human activity was the dominant cause (75%). An approximate 50–50% was observed in the last decade, with 94% of the lightning-caused wildfires occurring in the last 5 years (2015–2019) (Fig. 5). The higher occurrence of large lightning-caused wildfires (Fig. 3) is because these wildfires are often remote and hence less accessible.

Approximately 58% and 42% of the spread events ($n = 212$) are associated with lightning- and human-caused wildfires respectively. The frequency of 1-, 2-, 3- and 4-day human- and lightning-caused associated spread events is shown in Fig. 8. Human-caused wildfires have a higher frequency of 4 spread days compared with lightning-caused wildfires, which have a higher frequency of 2–3 spread days. There is, however, no significant difference in their distributions (K-S test not significant at $\alpha = 0.05$).

Fire danger analysis

Table 3 summarises the median ($\tilde{x}$), maximum (max) and bootstrap 95% confidence interval (CI) for FFMC, ISI and Buildup Index (BUI) by cause and period for the spread day events. BUI is a numerical rating of the amount of fuel available for consumption that provides an indication of the difficulty to contain a wildfire. The distributions of FFMC, ISI and BUI for all categories in Table 3 except Period 1 (1990–2004) and Period 2 (2005–2019) for human-caused wildfire spread day events failed the Shapiro–Wilk normality test ($\alpha = 0.05$). Median values were therefore calculated and a bootstrap with replacement used to estimate their 95% CI. If the confidence intervals for the compared medians did not overlap, we concluded there was a significant statistical difference between the medians of the two distributions (Table 3).

The median FFMC for all spread day events for the 1990–2019 period is very high (91), as shown in Table 1. The median ISI is also very high (16.8). The median BUI is in the high category (48). Therefore, while the spread events are characterised by very high and extreme FFMC and ISI values, very high to extreme BUI is not a prerequisite for large spring wildfires in Alberta. For example, in 2011, BUI values for the daily spread events ranged from 8 to 134. Snow patches were still evident the day before Wildfire SWF-065–2011 burned through the town of Slave Lake. On 14 May, the nearby S2 automatic weather station reported a BUI of 20 (low category).

FFMC has narrower categorical ranges (e.g. Very High 89–91) compared with ISI and BUI, and is the only FWI not open-ended. FFMC ranges from 0 to 99 and has a maximum probable value of 96 (de Groot 1987). The maximum value observed for all 212 spread day events was 96.4. FFMC values ≥94 were only observed in the second period (2005–2019).

As well, these extreme FFMC values only occurred when the relative humidity (RH) was very low or extreme ($n = 24$, $\bar{x}$ RH = 21%). Significant increases in the mean median FFMC for lightning-, human- and all-caused wildfires occurred from Period 1 to Period 2. Median ISI increased from Period 1 to Period 2 for lightning-caused wildfires. Human-caused wildfires had a higher median ISI (16.7) compared with lightning-caused wildfires for the entire period (1990–2019).

Table 4 summarises the median ($\tilde{x}$), maximum and bootstrap median CIs for FFMC, ISI and BUI by cause and period for the non-spread day events ($n = 108$) during the first 4 days. The median FFMC for all non-spread day events for the 1990–2019 period is high (87). The difference compared with the very high FFMC (91) for the spread day events is statistically significant. The median ISI for the non-spread day events is moderate (4.4) compared with the very high median ISI for the spread day events (13.7).

The median BUI values for spread (47.5) and non-spread (45) day events are not statistically different. However, the median

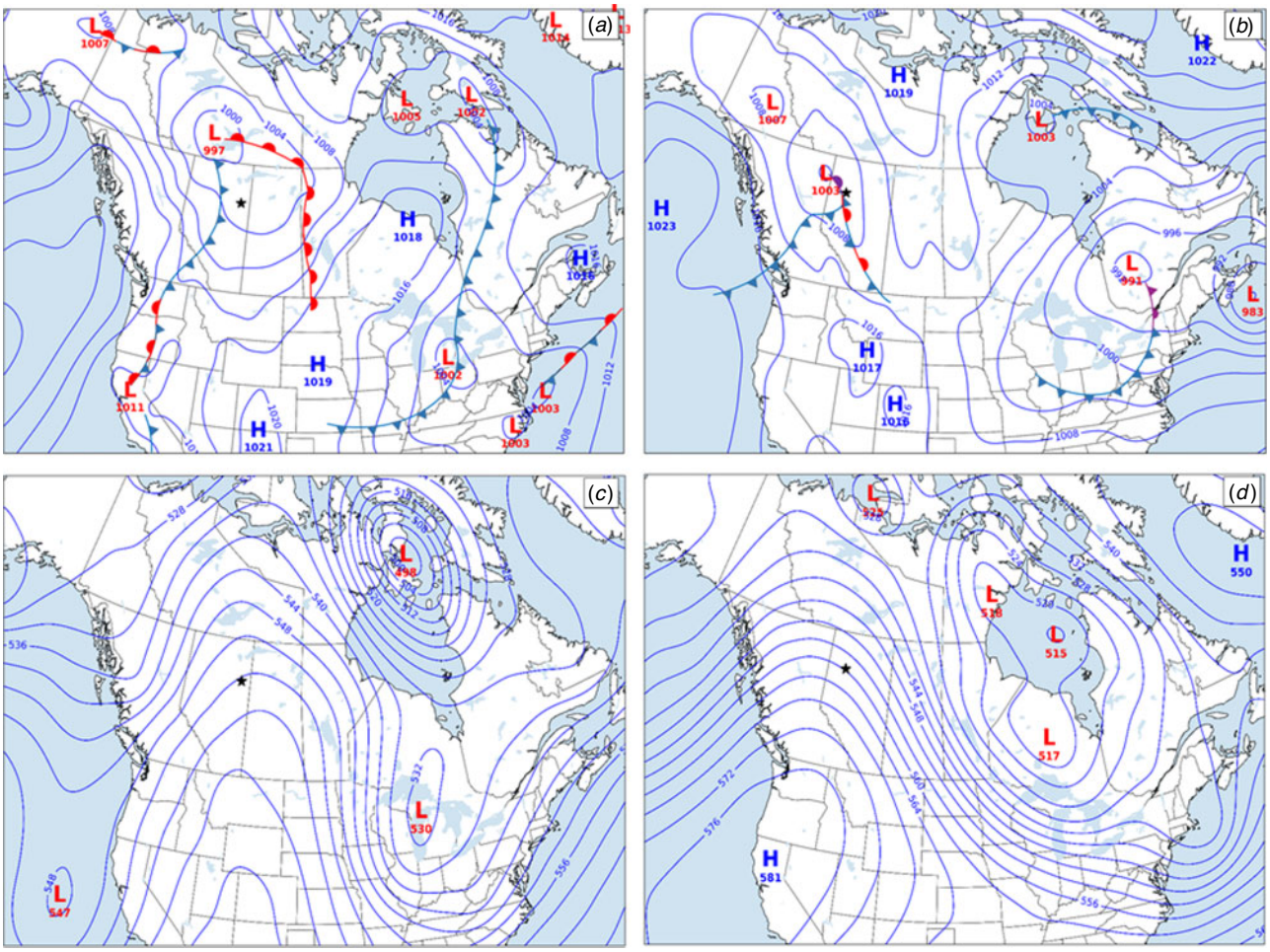

Fig. 6. Surface and 500 hPa analysis on 4 May 2016 (*a*, surface map; *c*, 500-hPa map), and 17 May 2008 (*b*, surface map; *d*, 500-hPa map). Surface maps are 1200 MDT (map *a*) and 1800 MDT (map *b*), and 500-hPa maps are 0600 MDT. The black star represents the Fort McMurray Urban Service Area (maps *a* and *c*), and Wildfire PWF019–2008 (maps *b* and *d*). Surface and 500-hPa maps are based on ERA5 model output. Fronts are delineated on the surface maps.

BUI value is statistically different between Periods 1 and 2 for all causes and lightning-caused alone.

Discussion

May wildfire starts resulted in structural losses from wildfires in 2001 (60 structures including 10 homes), 2011 (456 homes and 23 non-residential building), 2016 (2400 homes and commercial structures) and 2019 (16 homes). Spring is a potentially dangerous wildfire season, in part because the live foliar moisture content is at a minimum just before the emergence of new coniferous tree needles when non-structural carbohydrates stored in the roots are translocated to support needle growth (Jolly *et al.* 2014). This seasonal change in foliar density and hence relative foliar moisture content occurs before the surge in photosynthetic spring recovery.

Referred to as the 'spring dip', this short phenomenon occurs after snow melt, and before green-up. Hirsch (1996) showed dates of the minimum foliar moisture content (~85%) across Canada as calculated by the Canadian Forest Fire Danger Rating System (CFFDRS). When Wildfire MWF-009–2016 ran into Fort McMurray on 4 May, the forest was just starting to green up. Wildfire management staff also observed the same phenology when Wildfire SWF-065–2011 entered the town of Slave Lake on 15 May 2011.

Air masses originating in northern Canada are dry in the spring because water bodies are frozen and there is little to no plant photosynthesis, and hence minimal transpiration feeding moisture into the atmosphere. Photosynthetic capacity is inhibited when temperatures drop below –7°C (Sevanto *et al.* 2006). When fine fuels such as surface litter, leaves, mosses, needles and twigs (<1 cm diameter) reach moisture content levels of ≤12% (FFMC ≥ 89), the ISI becomes very responsive to small changes in the wind speed (Lawson and Armitage 2008).

During our exploratory analysis of the weather data, we noted the occurrence of days when our estimated ISI value using ERA5 weather outputs was less than 9 but significant wildfire growth was reported. Gusts occurred on these days. Incorporating gusts to support wildfire preparedness and suppression planning is particularly challenging. Wildfire modelling typically inputs the 10-min average wind speed of the last

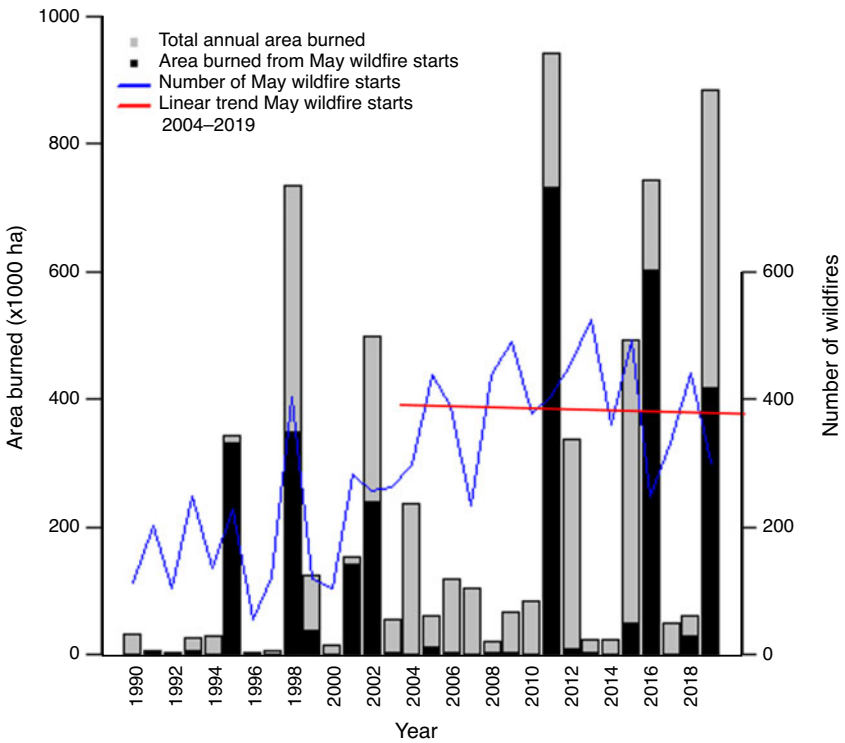

Fig. 7. Area burned from May wildfire starts compared with total annual area burned and number of May wildfires starts with a linear trend line for the 2004–2019 period (reporting procedure changed in 2004, resulting in an increase in reported wildfires).

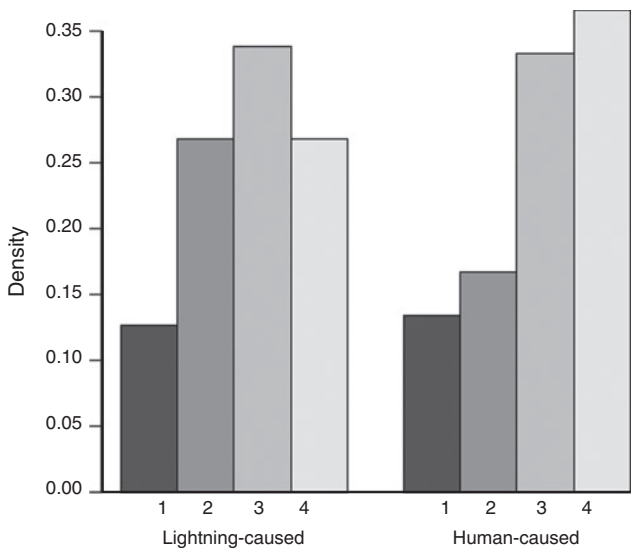

Fig. 8. Distribution of 1-, 2-, 3- and 4-day spread events for human- and lightning-caused wildfires starting in May and exceeding 1000 ha in size.

10 min before the hour. If the gust wind speed is used, the modelled wildfire growth will likely be overpredicted. Likewise, if the 10-min average wind speed is used and turbulence and gusts occur, the modelled output will likely be underpredicted (Scott 2012).

Since ISI responds non-linearly to wind speed, short periods (e.g. 1-min average of samples taken every 0.25 s) of high wind speed have more impact on wildfire behaviour than longer averaged periods (e.g. standard 10-min average of 0.25 s samples). Short periods of gusts can potentially generate firebrands and initiate crowning (Scott 2012).

We consider the approach described by Crosby and Chandler (2004) and its use by wildfire behaviour analysts to predict wildfire behaviour (Scott 2012) as reasonable in the absence of empirical data on the behaviour of gusts, and in particular, the frequency and timing of these gusts. In Alberta, the reported gust is the peak gust during the hour. Periods of gusts associated with a frontal passage are typically of short duration whereas periods of gusts associated with a pressure gradient force can be sustained during the day and night.

We observed an underestimation of mean wind speeds of 0.8 m s^{-1} (1 km h^{-1}) in the ERA5 reanalysis. This may have caused a negative bias in ISI values and explains why the ISI ≥ 9 threshold was not reached for some days. Jourdier (2020) and Tetzner *et al.* (2019) also reported an underestimation of ERA5 wind speeds.

Overall, a relatively small percentage of days in the spring are wildfire spread event days in Alberta. Of the 92 calendar days when spread events from one or more wildfires occurred, approximately one-quarter experienced strong south–south-east winds associated with continental polar air masses. However, cold fronts are the predominant feature with approximately half of the calendar spread days having pre-frontal or frontal passage activity.

Table 3. Median ($\tilde{x}$), maximum (max) and bootstrap confidence intervals (CI) for FFMC, ISI and BUI by cause and period for the spread day events
The median FFMC, ISI and BUI denoted by paired superscript indicate significant differences between the medians

Spread day events	*n*	FFMC		ISI		BUI	
		$\tilde{x}$ 0.95 CI	Max	$\tilde{x}$ 0.95 CI	Max	$\tilde{x}$ 0.95 CI	Max
All (1990–2019)	212	91 90.0–91.0	96.4	13.7 12.5–15.2	68.4	47.5 43.5–51.5	132
All lightning-caused wildfires (1990–2019)	127	91 90.0–91.0	95	12.2[d] 11.0–13.5	30.3	49 42.0–53.0	132
All human-caused (1990–2019)	85	92 90.7–92	96.4	16.7[d] 14.6–22.0	68.4	46 38.0–46.0	102
Period 1 (1990–2004) All	104	90[a] 88.1–90.0	93	13.2 11.2–15.1	68.4	41[f] 35.0–45.0	92
Period 2 (2005–2019) All	108	92.3[a] 91.9–93.0	96.4	14.1 12.5–15.8	53.7	53[f] 48.0–58.5	132
Period 1 (1990–2004) lightning-caused	85	90[b] 89.0–90.0	93	12.7[e] 10.8–14.3	30.3	38[g] 33.0–42.0	83
Period 2 (2005–2019) lightning-caused	42	92[b] 90.7–92.0	95	17.8[e] 14.3–25.95	29	84[g] 67.0–92.0	132
Period 1 (1990–2004) human-caused	19	90[c] 87.0–90.0	93	16.6 9.6–25.7	68.4	53 35.0–58.0	92
Period 2 (2005–2019) human-caused	66	92[c] 90.7–92.0	96.4	17.8 14.4–25.6	53.7	46 29.0–49.0	102

Table 4. Median ($\tilde{x}$), maximum (max) and bootstrap and confidence intervals (CI) for FFMC, ISI and BUI by cause and period for the non-spread day events
The median BUI denoted by paired superscript indicates significant differences between the medians

Non-spread day events	*n*	FFMC		ISI		BUI	
		$\tilde{x}$ 0.95 CI	Max	$\tilde{x}$ 0.95 CI	Max	$\tilde{x}$ 0.95 CI	Max
All (1990–2019)	108	87 82.6–87.0	93	4.4 3.7–5.0	26.1	45 41.0–50.5	134
All lightning-caused wildfires (1990–2019)	77	86 82.0–87.0	93	4.4 3.2–5.0	18.2	43 35.0–46.0	134
All human-caused (1990 –2019)	31	87 77.0–87.5	93	4.8 2.4–5.8	26.1	50 41.0–59.0	89
Period 1 (1990–2004) All	60	85 79.5–87.0	93	4.4 3.0–5.0	18.2	38.5[a] 34.0–43.0	89
Period 2 (2005–2019) All	48	87 81.0–88.0	93	4.6 2.7–5.5	26.1	57[a] 47.5–68.0	134
Period 1 (1990–2004) lightning-caused	47	83 78.0–87.0	93	4.4 3.1–5.1	18.2	35[b] 30.9–38.0	74
Period 2 (2005–2019) lightning-caused	30	87 81.0–89.0	93	4.3 2.1–5.5	8.6	68.5[b] 52.0–80.0	134
Period 1 (1990–2004) human-caused	13	87 77.0–87.5	90	4.4 1.7–5.1	8.2	66 39.0–69.0	89
Period 2 (2005–2019) human-caused	18	87.5 78.0–89.0	93	5.0 1.8–6.5	26.1	47.5 37.0–56.0	82

While the synoptic weather patterns associated with strong south–south-east winds were less frequent than the cold front synoptic weather pattern, they resulted in unique challenges, including night-time burning and the inability to conduct aerial suppression operations due to the very high to extreme winds. During the 18–25 May period in 1968, strong, dry south-easterly winds persisted all day and night, which desiccated vegetation and contributed to the extreme wildfire behaviour (McLean and Coulcher 1968). Fire behaviour analysts need to understand and account for the cumulative impact of sustained strong, dry winds because live fuel moisture other than conifer foliar moisture is not directly accounted for in the FWI. As well, the daily FWI

outputs use a standard daylength and diurnal curves for temperature, relative humidity and wind speed. These curves assume there is a night-time recovery period.

Strong, desiccating winds can also dry fuels before a wildfire starts. In 2011, 3 days of dry south-east winds occurred on 7–9 May, and again, but more strongly on 11–13 May, before the wildfire outbreak on 14 May when Wildfire SWF-65–2011 ran into the town of Slave Lake. In 2015, strong, dry south-east winds occurred 11–19 May 2015 before the wildfire outbreak started on 22 May.

In the CFFDRS, the Drought Code (DC) provides an indication of the moisture content of deep organic layers, and the difficulty of extinguishing a wildfire. DC is an input to BUI. Our analysis suggests drought is not a prerequisite for extreme wildfire behaviour during the spring season in Alberta. Very high (61–89) or extreme BUI (≥90) occurred on 30% (64) of the 212 spread day events. Our results indicate that spring wildfires in Alberta are primarily ISI driven.

Although outside the scope of our study, a more thorough investigation of our dataset is required to assess whether atmospheric stability and occurrence of low-level jets were contributing factors to extreme wildfire behaviour. The position of the polar jet stream relative to the location of wildfires is also an area of further study since the jet stream influences synoptic weather patterns.

Conclusion

The small percentage of wildfire spread days in the spring is associated with critical synoptic weather patterns. The predominant surface weather feature contributing to extreme wildfire behaviour on these spread days is the cold front passage (48%). Strong south–south-east winds resulting from a surface high or ridge positioned west of Hudson Bay occurred on 26% of the wildfire spread days.

Human-caused wildfires in the spring cause the greatest structural losses. Wildfire management agencies have a suite of prevention tools to help reduce the risk of these wildfires. Fire bans and restrictions, forest area closures and off-highway vehicle restrictions can be effective, but they need to be strategically applied and removed quickly. In Canada, a program called FireSmart promotes a shared responsibility to build wildfire-resilient communities. The seven disciplines of this program (education, vegetation management, emergency planning, legislation, development, interagency cooperation and cross-training) contribute to both mitigation and prevention of wildfire. Unfortunately, FireSmart practices across Canada are underutilised to help mitigate structure losses from spring wildfires.

Canada's Changing Climate Report (Government of Canada 2019) states warming in Canada will on average continue at more than twice the average global warming rate. Managing spring wildfires to protect multiple and competing values at risk is becoming more challenging because of climate change impacts including extended wildfire seasons (Jolly *et al.* 2015; Jain *et al.* 2017), increased extreme fire weather (Flannigan *et al.* 2016; Wang *et al.* 2016), increased area burned (Flannigan *et al.* 2005; Hanes *et al.* 2019), increased wildfire occurrence (Wotton *et al.* 2010) and reduced suppression capability (Podur and Wotton 2010; Wotton *et al.* 2017).

Spring wildfires with very high BUI values require more suppression effort to contain them because larger-diameter dead and downed fuels and deeper organic fuels are available for combustion. High average BUI values were observed in 2019, and very high BUI values in 2015 and 2018 during May. Very high to extreme BUI, however, is not a prerequisite for extreme wildfire behaviour. The common drivers for extreme wildfire behaviour in the spring are very high to extreme FFMC and ISI. Because spring wildfires in Alberta are wind-driven, extreme wildfire behaviour can occur quickly and become very challenging to manage.

We observed a significant increase in ISI from Period 1 to Period 2 for lightning wildfires, due in part to higher FFMC values in Period 2. BUI also increased from Period 1 to Period 2 for lightning wildfires, suggesting a drier boreal forest in the future will result in more lightning starts. The increasing trend in large lightning-caused wildfires in Alberta's boreal forest during the 2015–2019 period may be linked to climate change. Our results provide a foundation for future work to help understand climate change impacts on wildfire activity. This includes changes in spring oceanic–atmospheric patterns (El Niño Southern Oscillation and Pacific Decadal Oscillation) that impact temperature, lightning occurrence and lightning wildfire arrivals.

Research is also required on wind extremes and the variability in wind speeds associated with gusts. New approaches to adjust wind speeds when gusts are forecast are needed to support wildfire operations. Prediction of wind events was identified as a key research area (Flat Top Complex Wildfire Review Committee 2012).

Understanding the relationship between weather patterns at the surface and aloft, and the observed wildfire behaviour is critical for preparedness and the ability to make 5-day and longer forecasts of the wildfire environment. Wildfire behaviour analysts need a better understanding of the synoptic weather patterns responsible for extreme wildfire behaviour. This, however, requires stronger linkages and integration between fire weather forecasters and fire behaviour analysts.

Our results suggest wildfires will continue to escape suppression efforts to contain them as they become larger and more intense owing to climate variability and change. Albertans therefore need to prepare and learn to live and work in a landscape with more wildfire.

Data availability

Alberta historical wildfire report data are available publicly at https://wildfire.alberta.ca/resources/default.aspx. Weather and Canadian FWI System indices from the Alberta Forestry Division weather station network are available via request to the WMB in Edmonton, Alberta at WF.AWCC-Weather@gov.ab.ca. The ERA5 high-resolution reanalysis of the Canadian FWI System indices are available at https://doi.org/10.5281/zenodo.3626193 (McElhinny *et al.* 2020). Archived North America surface and 500-hPa synoptic weather maps are available from the NOAA.

Conflicts of interest

Mike Flannigan is an Associate Editor of International Journal of Wildland Fire but was blinded from the peer-review process for this paper.

Declaration of funding

This research did not receive any specific funding.

Acknowledgements

We thank Alberta Agriculture and Forestry Wildfire Management Branch for providing wildfire report and weather data. We also thank the two anonymous reviewers for their constructive comments.

References

Beaubien E, Hamann A (2011) Spring flowering response to climate change between 1936 and 2006 in Alberta, Canada. *Bioscience* **61**, 514–524. doi:10.1525/BIO.2011.61.7.6

Brotak EA, Reifsnyder WE (1977) An investigation of the synoptic situations associated with major wildland fires. *Journal of Applied Meteorology* **16**, 867–870. doi:10.1175/1520-0450(1977)016<0867:AIOTSS>2.0.CO;2

Byram GM (1954) Atmospheric conditions related to blowup fires. USDA Forest Service, Southeastern Forest Experiment Station, Paper No. 35. (Asheville, NC, USA).

Coogan SCP, Robinne F-N, Jain P, Flannigan MD (2019) Scientists' warning on wildfire – a Canadian perspective. *Canadian Journal of Forest Research* **49**, 1015–1023. doi:10.1139/CJFR-2019-0094

Crimmins M (2006) Synoptic climatology of extreme fire weather conditions across the southwest United States. *International Journal of Climatology* **26**, 1001–1016. doi:10.1002/JOC.1300

Crosby JS, Chandler CC (2004) Get the most from your windspeed observation. *Fire Management Today* **64**, 53–55.

Cumming SG (2001) Forest type and wildfire in the Alberta boreal mixedwood: What do fires burn? *Ecological Applications* **11**, 97–110. doi:10.1890/1051-0761(2001)011[0097:FTAWIT]2.0.CO;2

de Groot WJ (1987) Interpreting the Canadian Forest Fire Weather Index (FWI) System. In 'Proceedings: Fourth Central Regional Fire Weather Committee Scientific and Technical Seminar', 2 April 1987, Winnipeg, Manitoba. (Ed KG Hirsch) pp. 3–14. Canadian Forestry Service, Northern Forestry Centre. (Edmonton, AB, Canada)

Duane A, Brotons L (2018) Synoptic weather conditions and changing fire regimes in a Mediterranean environment. *Agricultural and Forest Meteorology* **253–254**, 190–202. doi:10.1016/J.AGRFORMET.2018.02.014

Flannigan MD, Harrington JB (1988) A study of the relation of meteorological variables to monthly provincial area burned by wildfire in Canada (1953–80). *Journal of Applied Meteorology* **27**, 441–452. doi:10.1175/1520-0450(1988)027<0441:ASOTRO>2.0.CO;2

Flannigan MD, Logan KA, Amiro BD, Skinner WR, Stocks BJ (2005) Future area burned in Canada. *Climatic Change* **72**, 1–16. doi:10.1007/S10584-005-5935-Y

Flannigan M, Stocks B, Turetsky M, Wotton W (2009) Impacts of climate change on fire activity and fire management in the circumboreal forest. *Global Change Biology* **15**, 549–560. doi:10.1111/J.1365-2486.2008.01660.X

Flannigan MD, Wotton BM, Marshall GA, de Groot WJ, Johnston J, Jurko N (2016) Fuel moisture sensitivity to temperature and precipitation: climate change implications. *Climatic Change* **134**, 59–71. doi:10.1007/S10584-015-1521-0

Flat Top Complex Wildfire Review Committee (2012) 2011 Flat Top Complex Wildfire Review in Alberta. Final report submitted to the Minister of Environment and Sustainable Resource Development, May 2012. Available at https://open.alberta.ca/publications/9781460102732 [Verified 8 February 2013]

Ganteaume A, Jappiot M (2013) What causes large fires in Southern France. *Forest Ecology and Management* **294**, 76–85. doi:10.1016/J.FORECO.2012.06.055

Government of Canada (2019) Canada's changing climate report. Environment and Climate Change Canada Report. (Eds E Bush, DS Lemmen) (Ottawa, ON, Canada) Available at https://changingclimate.ca/CCCR2019

Government of Canada (2021) Historical data. Environment and Climate Change (Ottawa, ON, Canada) Available at https://climate.weather.gc.ca/historical_data/search_historic_data_e.html

Hanes CC, Wang X, Jain P, Parisien M-A, Little JM, Flannigan MD (2019) Fire-regime changes in Canada over the last half century. *Canadian Journal of Forest Research* **49**, 256–269. doi:10.1139/CJFR-2018-0293

Hirsch K (1996) Canadian Forest Fire Behaviour Prediction (FBP) System: user's guide. Natural Resources Canada, Canadian Forest Service Special Report 7. (Edmonton, AB, Canada)

Jain P, Wang X, Flannigan MD (2017) Trend analysis of fire season length and extreme fire weather in North America between 1979 and 2015. *International Journal of Wildland Fire* **26**, 1009–1020. doi:10.1071/WF17008

Jolly WM, Hadlow AM, Huguet K (2014) De-coupling seasonal changes in water content and dry matter to predict live conifer foliar moisture content. *International Journal of Wildland Fire* **23**, 480–489. doi:10.1071/WF13127

Jolly WM, Cochrane MA, Freeborn PH, Holden ZA, Brown TJ, Williamson GJ, Bowman DMJS (2015) Climate-induced variations in global wildfire danger from 1979 to 2013. *Nature Communications* **6**, 7537. doi:10.1038/NCOMMS8537

Jourdier B (2020) Evaluation of ERA5, MERRA-2, COSMO-REA6, NEWA and AROME to simulate wind power production over France. *Advances in Science and Research* **17**, 63–77. doi:10.5194/ASR-17-63-2020

Kiil AD, Grigel JE (1969) The May 1968 conflagrations in central Alberta: A review of fire weather, fuels and fire behavior. Forestry Branch, Forest Research Laboratory Information Report A-X-24. (Edmonton, AB, Canada)

Kirchmeier-Young MC, Zwiers FW, Gillett NP, Cannon AJ (2017) Attributing extreme fire risk in western Canada to human emissions. *Climatic Change* **144**, 365–379. doi:10.1007/S10584-017-2030-0

Krawchuk MA, Cumming SG, Flannigan MD, Wein RW (2006) Biotic and abiotic regulation of lightning fire initiation in the mixedwood boreal forest. *Ecology* **87**, 458–468. doi:10.1890/05-1021

Lagerquist R, Flannigan MD, Wang X, Marshall GA (2017) Automated prediction of extreme fire weather from synoptic patterns in Northern Alberta, Canada. *Canadian Journal of Forest Research* **47**, 1175–1183. doi:10.1139/CJFR-2017-0063

Lawson BD, Armitage OB (2008) Weather guide for the Canadian Forest Fire Danger Rating System. Natural Resources Canada, Canadian Forest Service, Northern Forestry Centre Report. (Edmonton, AB, Canada).

McElhinny M, Beckers JF, Hanes C, Flannigan M, Jain P (2020) A high-resolution reanalysis of global fire weather from 1979 to 2018 – overwintering the Drought Code. *Earth System Science Data* **12**, 1823–1833. doi:10.5194/ESSD-12-1823-2020

McLean J, Coulcher B (1968) Seven days in May: Meteorological factors associated with Alberta forest fires of May 18–25, 1968. Alberta Energy and Natural Resources, Forest Service Report. (Edmonton, AB, Canada)

Mesinger F, Dimego G, Kalnay E, Mitchell K, Shafran P, Ebisuzaki W, Jović D, Woollen J, Rogers E, Berbery E, Ek M, Fan Y, Grumbine R, Higgins W, Li H, Lin Y, Manikin G, Parrish D, Wei S (2006) North American regional reanalysis. *Bulletin of the American Meteorological Society* **87**, 343–360. doi:10.1175/BAMS-87-3-343

Met Office (2021) Cartopy: A cartographic python library with a matplotlib interface (v0.18.0). Available at https://scitools.org.uk/cartopy (Exter, Devon, UK)

National Oceanic and Atmospheric Administration (2021*a*) Surface analysis archive. Available at https://www.wpc.ncep.noaa.gov/archives/web_pages/sfc/sfc-zoom.html. [Verified 30 June 2021]

National Oceanic and Atmospheric Administration (2021*b*) Central library weather and climate collections. Available at https://library.noaa.gov/Collections/Digital-Collections/US-Daily-Weather-Maps. [Verified 30 June 30 2021]

National Oceanic and Atmospheric Administration (2021*c*) Surface analysis archive. Available at https://www.wpc.ncep.noaa.gov/archives/web_pages/sfc/sfc_archive.php. [Verified 30 June 2021]

National Oceanic and Atmospheric Administration (2021*d*) Daily weather map. Available at https://www.wpc.ncep.noaa.gov/dailywxmap/index.html. [Verified 30 June 2021]

Nimchuk N (1983) Wildfire behavior associated with upper ridge breakdown. Alberta Energy and Natural Resources, Forest Service Report No. T/50. (Edmonton, AB, Canada)

Parente J, Pereira MG, Tonini M (2016) Space–time clustering analysis of wildfires: The influence of dataset characteristics, fire prevention policy decisions, weather and climate. *The Science of the Total Environment* **559**, 151–165. doi:10.1016/J.SCITOTENV.2016.03.129

Parisien M-A, Walker GR, Little JM, Simpson BN, Wang X, Perrakis DDB (2013) Considerations for modeling burn probability across landscapes with steep environmental gradients: an example from the Columbia Mountains, Canada. *Natural Hazards* **66**, 439–462. doi:10.1007/S11069-012-0495-8

Parks SA, Holsinger LM, Panunto MH, Jolly WM, Dobrowski SZ, Dillon GK (2018) High-severity fire: evaluating its key drivers and mapping its probability across western US forests. *Environmental Research Letters* **13**, 044037. doi:10.1088/1748-9326/AAB791

Pereira MG, Trigo RM, Camara CD, Pereira JMC (2005) Synoptic patterns associated with large summer forest fires in Portugal. *Agricultural and Forest Meteorology* **129**, 11–25. doi:10.1016/J.AGRFORMET.2004.12.007

Pickell PD, Coops NC, Ferster CJ, Bater CW, Blouin KD, Flannigan MD (2017) An early warning system to forecast the close of the spring burning window from satellite-observed greenness. *Scientific Reports* **7**, 14190. doi:10.1038/S41598-017-14730-0

Podur J, Wotton BM (2010) Will climate change overwhelm fire management capacity? *Ecological Modelling* **221**, 1301–1309. doi:10.1016/J.ECOLMODEL.2010.01.013

Podur J, Wotton BM (2011) Defining fire spread event days for fire-growth modelling. *International Journal of Wildland Fire* **20**, 497–507. doi:10.1071/WF09001

Python Software Foundation (2021) Python Language Reference, version 3.8.10. Available at https://www.python.org

R Core Team (2020) R: A language and environment for statistical computing. R Foundation for Statistical Computing. (Vienna, Austria)

Ruffault J, Moron V, Trigo RM, Curt T (2017) Daily synoptic conditions associated with large fire occurrence in Mediterranean France: evidence for a wind-driven fire regime. *International Journal of Climatology* **37**, 524–533. doi:10.1002/JOC.4680

Schaefer VJ (1957) The relationship of jet streams to forest wildfires. *Journal of Forestry* **55**, 419–425.

Schroeder MJ, Glovinsky M, Hendricks VF, Hood FC, Hull MK, Jacobson HL, Kirkpatrick R, Krueger DW, Mallory LP, Oertel AG, Reese RH, Sergius LA, Syverson CE *et al*. (1964) Synoptic weather types associated with critical fire weather. USDA Forest Service, Pacific Southwest Forest and Range Experiment Station Report prepared for Office Civil Defense. (Berkeley, CA, USA)

Scott JH (2012) Introduction to Wildfire Behavior Modeling. National Interagency Fuels, Fire, and Vegetation Technology Transfer, USDA Forest Service, Rocky Mountain Research Station. (Fort Collins, CO, USA).

Sevanto S, Suni T, Pumpanen J, Gronholm T, Kolari P, Nikinmaa E, Hari P, Vesala T (2006) Wintertime photosynthesis and water uptake in a boreal forest. *Tree Physiology* **26**, 749–757. doi:10.1093/TREEPHYS/26.6.749

Skinner WR, Flannigan MD, Stocks BJ, Martell DL, Wotton BM, Todd JB, Mason JA, Logan KA, Bosch EM (2002) A 500 Mb synoptic wildland fire climatology from large Canadian forest fires, 1959–1996. *Theoretical and Applied Climatology* **71**, 157–169. doi:10.1007/S007040200002

Tetzner D, Thomas E, Allen C (2019) A validation of ERA5 reanalysis data in the southern Antarctic Peninsula – Ellsworth Land Region, and its implications for ice core studies. *Geosciences* **9**, 289. doi:10.3390/GEOSCIENCES9070289

Trouet V, Taylor AH, Carleton AM, Skinner CN (2009) Interannual variations in fire weather, fire extent, and synoptic-scale circulation patterns in northern California and Oregon. *Theoretical and Applied Climatology* **95**, 349–360. doi:10.1007/S00704-008-0012-X

Tymstra C (2015) 'The Chinchaga Firestorm: When the moon and sun turned blue.' (University of Alberta Press: Edmonton, AB, Canada)

Tymstra C, Woolford DG, Flannigan MD (2019) Statistical surveillance thresholds for enhanced situational awareness of spring wildland fire activity in Alberta, Canada. *Journal of Environmental Statistics* **9**(4), http://www.jenvstat.org/v09/i04/paper.

Tymstra C, Stocks BJ, Cai X, Flannigan MD (2020) Wildfire management in Canada: Review, challenges and opportunities. *Progress in Disaster Science* **5**, 100045. doi:10.1016/J.PDISAS.2019.100045

Van Wagner CE (1987) Development and structure of the Canadian Forest Fire Weather Index System. Government of Canada, Canadian Forest Service, Forestry Technical Report. (Ottawa, ON, Canada)

Verdú F, Salas J, Vega-Garcia C (2012) A multivariate analysis of biophysical factors and forest fires in Spain, 1991–2005. *International Journal of Wildland Fire* **21**, 498–509. doi:10.1071/WF11100

Viedma O, Quesada J, Torres I, De Santis A, Moreno JM (2015) Fire severity in a large fire in a *Pinus pinaster* forest is highly predictable from burning conditions, stand structure, and topography. *Ecosystems* **18**, 237–250. doi:10.1007/S10021-014-9824-Y

Wang X, Parisien M-A, Taylor SW, Perrakis DDB, Little J, Flannigan MD (2016) Future burn probability in south-central British Columbia. *International Journal of Wildland Fire* **25**, 200–212. doi:10.1071/WF15091

Wiken EB (1986) Terrestrial Ecozones of Canada. Ecological Land Classification, Series No. 19. Environment Canada. (Hull, Quebec, Canada)

Wotton BM, Nock CA, Flannigan MD (2010) Forest fire occurrence and climate change in Canada. *International Journal of Wildland Fire* **19**, 253–271. doi:10.1071/WF09002

Wotton BM, Flannigan MD, Marshall GA (2017) Potential climate change impacts on fire intensity and key wildfire suppression thresholds in Canada. *Environmental Research Letters* **12**, 095003. doi:10.1088/1748-9326/AA7E6E

Zhong S, Yu L, Heilman WE, Bian X, Fromm H (2020) Synoptic weather patterns for large wildfires in the northwestern United States – a climatological analysis using three classification methods. *Theoretical and Applied Climatology* **141**, 1057–1073. doi:10.1007/S00704-020-03235-Y